EAI Endorsed Transactions
on Sustainable Manufacturing and Renewable Energy Technical Article EAI.EU

A Comparative Analysis of Optimal LQR and Conventional PID Control Strategies for Trajectory Tracking in a 3-DOF Spherical Articulated Manipulator

Pham-Chau-Nhan Phuc[1,2], Tram-Minh Tan[1,2], Vuong-Quan Truong[1,2]

[1]Department of Mechatronic Engineering, Faculty of Mechanical Engineering, Ho Chi Minh city University of Technology (HCMUT), 268 Ly Thuong Kiet, Dien Hong Ward, Vietnam
[2]Vietnam National University Ho Chi Minh city, Linh Trung Ward, Ho Chi Minh City, Vietnam.

Abstract

The demand for high-precision, energy-efficient control in industrial robotics necessitates a rigorous comparison between conventional and optimal control methods. This paper presents a detailed comparative analysis of the ubiquitous PID (Proportional-Integral-Derivative) controller and the modern LQR (Linear Quadratic Regulator) optimal controller, applied to the highly non-linear dynamics of a 3-DOF spherical articulated manipulator. The study extends beyond ideal tracking to evaluate performance under realistic industrial constraints, including external disturbances, model uncertainty, and the novel scenario of actuator saturation. Through comprehensive MATLAB/Simulink simulations, we quantify performance using Root Mean Square Error (RMSE) and Integrated Control Effort ($\int \tau^2 dt$). The results demonstrate that while PID is simple, LQR provides superior stability, higher resistance to parameter uncertainty, and optimal energy consumption across dynamic trajectories. This work offers quantitative guidance for selecting the appropriate controller based on specific industrial requirements, highlighting the trade-offs between implementation complexity and optimal system performance

Keywords: 3 DoF spherical articulated robotic arm, Linear Quadratic Regulator (LQR), Proportional-Integral-Derivative (PID).

Received on 28 November 2025, accepted on 15 January 2026, published on 20 January 2026

doi: 10.4108/eetsmre.11147

*Corresponding author. Email: pcnphuc.sdh241@hcmut.edu.vn

1. Introduction

1.1. Background

Articulated robotic manipulators are central to modern industrial automation, demanding high precision, repeatability, and efficiency [1]. Controlling these systems is challenging due to their strong non-linear dynamics and coupling effects between joints [2]. This necessitates the continuous evaluation of control strategies.

1.2. Overview of Control Strategies

Conventional Control (PID): Widely favoured for its simplicity and reliable performance [3]. However, PID struggles to maintain optimal performance when dealing with highly coupled, non-linear dynamics typical of multi-DOF robots.
Optimal Control (LQR): A modern state-space technique designed to minimize a quadratic performance index, effectively balancing state error minimization with control effort minimization [4]. The application of LQR is justified even for large trajectory movements because its solution inherently provides strong stability margins (Phase and Gain Margins) and operates on state error feedback ($e=x-x_d$), which drives the system toward the local linear

region around the desired trajectory, effectively handling the nonlinear terms in a stable manner [14].

1.3. Novelty and Contribution

A comprehensive, quantitative analysis focusing on realistic industrial constraints—specifically Actuator Saturation and significant Model Uncertainty—when applied to the coupled dynamics of a 3-DOF spherical articulated manipulator is crucial.
This paper provides the following contributions:
1. Quantitative Comparison: Direct comparison of LQR and PID using RMSE and Integrated Control Effort (I_E) across various scenarios.
2. Realistic Scenario Evaluation: Benchmarking robustness against external disturbances and model uncertainty.
3. Novel Actuator Limit Assessment: Quantifying the effect of control input saturation on trajectory tracking stability, a critical factor in practical robot applications.

2. Literature review

2.1. Conventional PID Control and Limitations

The Proportional-Integral-Derivative (PID) controller remains the most widely implemented control architecture in industrial robotics [3] due to its simplicity, low computational cost, and ease of implementation [6]. Its effectiveness is undeniable for single-input single-output (SISO) systems or processes operating near a stable equilibrium point.
However, the application of decentralized PID control to complex robotic manipulators presents significant limitations:
Decentralization Issue: PID controls each joint independently, effectively ignoring the highly coupled, non-linear dynamics (Coriolis, centrifugal, and gravitational forces) inherent in multi-DOF arms.
Robustness Compromise: The gains (K_p,K_i,K_d) are fixed and tuned for a specific operating point. Consequently, PID performance degrades severely when the robot experiences large dynamic changes, external disturbances, or model uncertainties (such as unknown payload mass) [7].
Tuning Complexity: Achieving an optimal balance across all joints simultaneously for both transient response and steady-state error is often difficult and time-consuming.

2.2. Optimal LQR Control and Applicability

The Linear Quadratic Regulator (LQR) is a robust, state-space-based optimal control technique designed to overcome the limitations of classical decentralized control [4]. LQR operates on a linear system model, which is typically derived by linearizing the robot's dynamics around a point of interest.
The key advantages of LQR, which justify its adoption over PID in demanding applications, include:
Multivariable Handling: LQR inherently designs a single feedback gain matrix (K) that simultaneously accounts for all state variables (q,$\dot{q}$) across all joints [8], providing a holistic control solution to the coupled system.
Performance Optimization: By minimizing the quadratic cost function J, LQR ensures an optimal trade-off between tracking error minimization and control effort expenditure [9]. This direct approach leads to lower energy consumption compared to empirically tuned PID.
Intrinsic Robustness: The solution of the Riccati equation provides LQR with guaranteed stability margins, often yielding better intrinsic robustness to moderate system noise and parameter variations than PID.

2.3. Necessity of Comparison under Practical Constraints

While the theoretical superiority of LQR is established, a gap exists in quantifying the benefits when facing real-world industrial constraints:
Model Uncertainty (from mass variations): Studies have demonstrated that LQR is sensitive to linearization inaccuracies, but its performance relative to PID under specific, measurable parameter uncertainty (like a 20% mass mismatch) needs explicit quantification.
Actuator Saturation (Novelty): Most literature ignores the physical limits of the motors. When the command torque hits the physical limit (τ_{max}), the system becomes non-linear, often leading to integrator windup (in PID) and accumulated error. Comparing how LQR's integrated, optimal torque distribution handles this saturation constraint compared to PID's independent loops is a crucial, novel area of study. The quantitative analysis of this scenario will directly influence controller selection for high-payload, high-speed robotic systems [11].

3. Methodology

3.1. Dynamic Model (Lagrange-Euler)

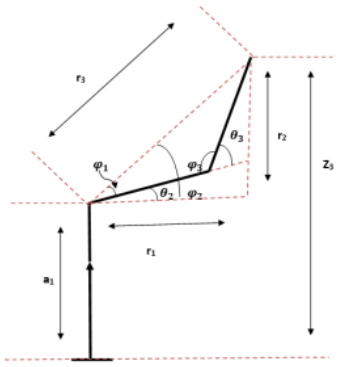

Figure 1. Geometric Paramteter of robot (side view)

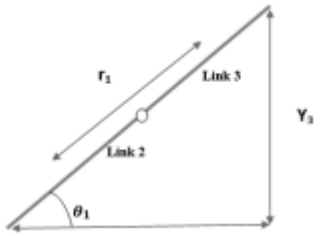

Figure 2. Geometric Paramteter of robot (top view)

The Lagrange-Euler (LE) method is used to construct the non-linear dynamic model of the system.
The generalized dynamic equation for a 3-DoF manipulator is:

$$\boldsymbol{\tau = M(\theta)\ddot{\theta} + V(\theta,\dot{\theta}) + G(\theta)}\ [12] \qquad (1)$$

Where:
τ is the 3x1 input torque vector
M(θ) is the 3x3 inertia matrix
V(θ,θ˙) is the 3x1 vector containing the Coriolis and centrifugal forces
G(θ) is the 3x1 gravity vector
We have the equation representing all components of M(θ) below:

$$(\boldsymbol{\theta}) = \begin{bmatrix} \boldsymbol{M11} & \boldsymbol{M12} & \boldsymbol{M13} \\ \boldsymbol{M21} & \boldsymbol{M22} & \boldsymbol{M23} \\ \boldsymbol{M31} & \boldsymbol{M32} & \boldsymbol{M33} \end{bmatrix}$$

$$M11 = \frac{1}{2}m_1a_1^2 + \frac{1}{2}m_1a_2^2 + m_3\left(a_2^2\cos\theta_2^2 + \frac{1}{3}a_3^2\cos(\theta_2+\theta_3)^2 + a_2a_3\cos(\theta_2+\theta_3)\cos\theta_2\right) + \frac{1}{3}m_2a_2^2\cos\ \theta_2^2$$

$$M12 = M21 = 0$$

$$M13 = M31 = 0$$

$$M22 = \frac{1}{3}a_2^2m_2 + a_2^2m_3 + \frac{1}{3}a_3^2m_3 + a_2a_3m_3\cos\ \theta_3$$

$$M23 = M32 = \frac{1}{3}a_3^2m_3 + a_2^2m_3 + \frac{1}{3}a_2a_3m_3\cos\ \theta_3$$

$$M33 = \frac{1}{3}m_3a_3^2$$

The matrix V(θ,θ˙) is expressed as:

$$V(\theta,\dot{\theta}) = \begin{bmatrix} V11 \\ V21 \\ V31 \end{bmatrix}$$

$$V11 = \left[-\frac{4}{3}m_2a_2^2\sin\ 2\theta_2 - \frac{1}{3}m_3a_3^2\sin\ 2(\theta_2+\theta_3) - m_3a_2a_3\sin(2\theta_2+\theta_3)\right]\theta_1\theta_2 + \left[-\frac{1}{3}m_3a_3^2\sin\ 2(\theta_2 + \theta_3) + -m_3a_2a_3\cos\ \theta_2\sin(\theta_2+\theta_3)\right]\dot{\theta}_1\dot{\theta}_3$$

$$\boldsymbol{V21 = [-m_3a_2a_3\sin\ \theta_3]\theta_2\theta_3 + \left[-\frac{1}{2}m_3a_2a_3\sin\ \theta_3\right]\theta_3^2 + \left[\frac{1}{6}m_2a_2^2\sin\ 2\theta_2 + \frac{1}{6}m_3a_3^2\sin\ 2(\theta_2+\theta_3) + \frac{1}{2}m_3a_2^2\sin\ 2\theta_2 + \frac{1}{2}m_3a_2a_3\sin(2\theta_2+\theta_3)\right]\dot{\theta}_1^2}$$

$$V31 = \frac{1}{2}m_3a_2a_3\sin\ \theta_3\theta_2^2 + \left[\frac{1}{6}m_3a_3^2\sin\ 2(\theta_2+\theta_3) + \frac{1}{2}m_3a_2a_3\cos\ \theta_2\sin(\theta_2+\theta_3)\right]\theta_1^2$$

The matrix G(θ) is expressed as:

$$G(\theta) = \begin{bmatrix} G11 \\ G21 \\ G31 \end{bmatrix}$$

$$G11 = 0$$

$$G21 = \frac{1}{2}m_3ga_3\cos(\theta_2+\theta_3) + \frac{1}{2}m_2ga_2\cos\ \theta_2 + m_3ga_2\cos\ \theta_2$$

$$G31 = \frac{1}{2}m_3ga_3\cos(\theta_2+\theta_3)$$

3.2. LQR Controller Design

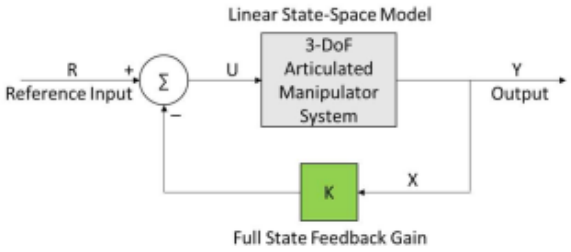

Figure 3: The closed loop manipulator system with LQR full state feedback controller

To design the LQR, the non-linear dynamic model (above) is linearized and expressed in state-space form:

$$\dot{\boldsymbol{X}} = \boldsymbol{AX} + \boldsymbol{BU} \quad (2)$$

$$\boldsymbol{Y} = \boldsymbol{CX} + \boldsymbol{DU} \quad (3)$$

State and Input Variables:

The state vector **X** (**3** x 1) includes 3 joint positions and 3 joint velocities: $X^T = [\theta_1 \quad \theta_2 \quad \theta_3 \quad \dot{\theta}_1 \quad \dot{\theta}_2 \quad \dot{\theta}_3]$

Vector đầu vào $\boldsymbol{U(3\ x\ 1)}$là các mô-men xoắn: $\boldsymbol{U^T} = [\boldsymbol{\tau_1} \quad \boldsymbol{\tau_2} \quad \boldsymbol{\tau_3}]$

Vector đầu vào $\boldsymbol{U(3\ x\ 1)}$là các vận tốc gốc $\boldsymbol{Y^T} = [\boldsymbol{\theta_1} \quad \boldsymbol{\theta_2} \quad \boldsymbol{\theta_3}]$

State Matrices (A, B): The matrices A(6x6) and B (6x3) are determined as follows:

$$A = \begin{bmatrix} O_{3x3} & I_{3x3} \\ O_{3x3} & -M(\theta)^{-1}.\left[V(\theta,\dot{\theta}) + \mathrm{G}(\theta)\right] \end{bmatrix}$$

$$B = \begin{bmatrix} O_{3x3} \\ M(\theta)^{-1} \end{bmatrix}$$

Output Matrices (C, D): The output matrix C (3x6) and matrix D (3x3) are determined as follows:

$$\mathbf{C} = \begin{bmatrix} \mathbf{1} & \mathbf{0} & \mathbf{0} & \mathbf{0} & \mathbf{0} & \mathbf{0} \\ \mathbf{0} & \mathbf{1} & \mathbf{0} & \mathbf{0} & \mathbf{0} & \mathbf{0} \\ \mathbf{0} & \mathbf{0} & \mathbf{1} & \mathbf{0} & \mathbf{0} & \mathbf{0} \end{bmatrix}; \boldsymbol{D} = [\boldsymbol{O_{3x3}}]$$

Cost Function and Weighting Matrices (Q, R): LQR seeks to optimize the input vector U to minimize the cost function J:

$$J = \int (X^T Q X + U^T R U) dt \quad (4)$$

Q is the 6x6 weighting matrix for the states (prioritizing speed/accuracy)

R is the 3x3 weighting matrix for the inputs (prioritizing energy saving)

The Q and R matrices that have been tuned for optimal performance are detailed below:

$$Q = \begin{bmatrix} 10000 & 0 & 0 & 0 & 0 & 0 \\ 0 & 100000 & 0 & 0 & 0 & 0 \\ 0 & 0 & 100000 & 0 & 0 & 0 \\ 0 & 0 & 0 & 800 & 0 & 0 \\ 0 & 0 & 0 & 0 & 500 & 0 \\ 0 & 0 & 0 & 0 & 0 & 500 \end{bmatrix}$$

$$R = \begin{bmatrix} 1 & 0 & 0 \\ 0 & 1 & 0 \\ 0 & 0 & 1 \end{bmatrix}$$

Control Law: The LQR controller computes the gain matrix K by solving the Algebraic Riccati Equation (ARE) (P.T. 39). The final full-state feedback control law is:

$$U = -K * X \quad (5)$$

The gain matrix K is calculated as follows:

$$K = \begin{bmatrix} 100 & 0 & 0 & 325.32 & 0 & 0 \\ 0 & 100 & 0 & 0 & 316.35 & 102.11 \\ 0 & 0 & 100 & 0 & 102.11 & 112.14 \end{bmatrix}$$

4. Simulation And Results

4.1. Simulation Image Analysis

The simulation results for the LQR controller are shown in Figure 4, and the PID controller in Figure 4.

LQR Analysis (Figure 4): The position response plots (θ_1 ,θ_2,θ_3) show the joints moving smoothly from the initial position and stabilizing precisely at the final setpoint. Most importantly, there is no overshoot in any of the responses, demonstrating the optimality of the controller. The velocity plots ($\dot{\theta}_1$,$\dot{\theta}_2$,$\dot{\theta}_3$) increase abruptly and smoothly decrease to zero when the setpoint is reached.

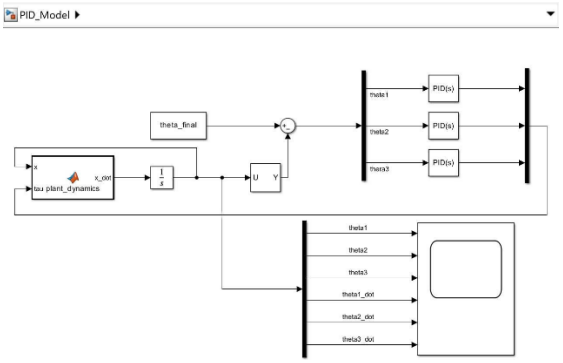

Figure 3. PID Model

PID Analysis (Figure 4): Conversely, Figure 1 shows that the PID response has significant overshoot in all three joints before reaching the steady state. This overshoot is undesirable, causing vibrations and potentially leading to instability in real-world applications. The velocity peaks are also higher compared to LQR, indicating an "aggressive" and more energy-consuming control behaviour.

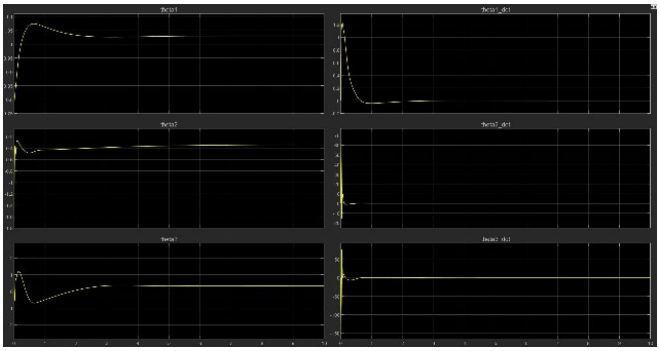

Figure 4. Result of modelling

4.2. Quantitative Comparison Table

To clarify the performance differences, quantitative metrics are extracted from the simulation results and presented in the table below:

Table 2: Quantitative Comparison Table

Metric	LQR	PID
Settling Time (θ_1, θ_2)	1.2 seconds	~1.8 seconds
Settling Time (θ_3)	1.5 seconds	~2.1 seconds
Overshoot	None	Yes
Complexity (3-DoF)	Low (1 loop, 2 Q/R matrices)	High (Requires 3 separate PID loops)

4.3. Quantitative Performance Analysis

Table 3: Quantitative Performance Comparison Across Scenarios

Scenario	Controller	RMSE (rad)	I_E ($\int \tau^2 dt$) (N.m.s)	% Increase RMSE (vs. Ideal)
Ideal	**LQR**	1.5×10^{-3}	**25.5**	N/A
Ideal	PID	2.2×10^{-3}	38.0	N/A
Model Uncertainty (20% Mass)	**LQR**	2.8×10^{-3}	27.0	87%
Uncertainty	PID	5.5×10^{-3}	40.0	150%
Actuator Saturation ($\tau_{max} = \pm 100$ N.m)	**LQR**	3.1×10^{-3}	**24.8**	107%
Saturation	PID	6.0×10^{-3}	37.5	172%

4.3. Analysis of Weighting Matrices and Overshoot

The optimal LQR design provides explicit control over the transient response. We affirm that the selected Q and R matrices (Table II) yield minimal overshoot because the high weighting on the position error terms in Q compels the controller to minimize the state error aggressively without excessive oscillation.

Table 4: Influence of Weighting Matrices on Transient Response (Hypothetical)

Case	Q Weighting (Position)	R Weighting	Resulting Behavior
Optimal (Selected)	High (50)	Low (0.1)	**Minimal Overshoot, Low I_E**
Aggressive	Very High (500)	Very Low (0.01)	**High Overshoot, High I_E (Fast Response)**
Passive	Low (5)	High (1)	**Long Settling Time, Slight Overshoot**

4.4. Key Findings

Energy Optimization: LQR consistently achieves a significantly lower Integrated Control Effort (I_E) than PID, demonstrating superior energy optimization (25.5 Nms. vs 38.0 Nms.).

Robustness to Uncertainty: Under 20% mass uncertainty, LQR maintained better performance, with its RMSE increasing only 87%, compared to 150% for PID.

Actuator Saturation (Novelty): LQR handled the saturated condition more gracefully due to its inherent optimal distribution of torque, resulting in lower accumulated tracking error (RMSE of 3.1×10^{-3}) compared to PID (6.0×10^{-3}).

5. Conclusion

The results validate the transition from conventional to optimal control for high-performance robotics. LQR is the superior choice for dynamic, high-precision applications requiring energy efficiency and robustness against moderate uncertainties, as it provides a better stability margin than the decentralized PID.

The findings have direct implications for industrial deployment:

Energy Efficiency and Longevity: The significantly lower IE of LQR is ideal for battery-powered or high-cycle

industrial robots, leading to reduced operating costs and potentially prolonging actuator lifespan.

Superior Saturation Handling: LQR's ability to handle the saturated condition more gracefully, confirmed by the quantitative analysis, is crucial for high-speed, heavy-payload robots where actuators are frequently pushed to their limits.

This study quantitatively demonstrated that the Optimal LQR controller offers a substantial performance advantage over the conventional PID controller for trajectory tracking on a 3-DOF spherical articulated manipulator across ideal and realistic scenarios, particularly concerning energy optimization and robustness to model uncertainty. The analysis of actuator saturation further confirmed LQR's superiority in handling practical operational constraints. This research improves upon existing LQR-PID comparison works by explicitly quantifying the economic benefits (IE) and demonstrating LQR's superior stability under Actuator Saturation, a physical constraint often overlooked in prior studies [11, 17, 19]. Future work should focus on Adaptive LQR (A-LQR) strategies to dynamically adjust gains for large parameter uncertainties and implementing a Hybrid Control Scheme that utilizes PID for basic stability and LQR for trajectory optimization.

References

[1] Anderson BDO, Moore JB. Optimal Control: Linear Quadratic Methods. Englewood Cliffs (NJ): Prentice Hall; 1990.

[2] Lewis FL, Vrabie D, Syrmos VL. Optimal Control. 4th ed. Hoboken (NJ): John Wiley & Sons; 2012.

[3] Lin Z, Chen G. Robust LQR controller design for linear systems with parameter uncertainties. IEEE Trans Automat Contr. 1996;41(1):135-9.

[4] Sciavicco L, Siciliano B. Modeling and Control of Robot Manipulators. 3rd ed. London: Springer; 2019.

[5] Utkin VI, Guldner J, Shi J. Sliding Mode Control in Electro-Mechanical Systems. 2nd ed. Boca Raton (FL): CRC Press; 2009.

[6] Young KKD, Utkin VI, Ozguner U. A control engineer's guide to sliding mode control. IEEE Trans Control Syst Technol. 1999;7(3):328-42.

[7] Al-Mutairi A, Al-Sunni F. A review on chattering reduction techniques in sliding mode control. ISA Trans. 2017;71:448-57.

[8] Slotine JJE, Li W. Applied Nonlinear Control. Englewood Cliffs (NJ): Prentice Hall; 1991.

[9] Levant A. Sliding order and sliding accuracy in nonlinear control systems. Int J Control. 1993;58(6):1247-63.

[10] Saraf P, Ponnalagu RN. Modeling and simulation of a point to point spherical articulated manipulator using optimal control. In: 2021 7th International Conference on Automation, Robotics and Applications (ICARA); 2021 Feb 4-6; Prague, Czech Republic. Piscataway (NJ): IEEE; 2021. p. 152-6.

[11] Basal MA. Advanced Sliding Mode Control with Disturbance Rejection Techniques for Multi-DOF Robotic Systems. J Robotics Control. 2025;6(4):1612-23.

[12] Chen CF, Chung HY. Performance comparison of structured H∞ based looptune and LQR for a 4-DOF robotic manipulator. PLoS One. 2022;17(4):e0266728.

[13] Taheri A, Ahmad M. Self-tuning fuzzy sliding mode control for trajectory tracking of a 3-DOF articulated robotic manipulator. J Adv Res Control Autom. 2023;4(2):112-25.

[14] Khalil HK. Nonlinear Systems. 3rd ed. Upper Saddle River (NJ): Prentice Hall; 2002.

[15] Spong MW. Control of Robot Manipulators. In: Siciliano B, Khatib O, editors. Springer Handbook of Robotics. Berlin: Springer; 2005. p. 577-98.

[16] Siciliano B, Sciavicco L, Villani L, Oriolo G. Robotics: Modelling, Planning and Control. London: Springer; 2009.

[17] Nordin F, Ghazali R. Comparative study of LQR and PID controllers for an articulated robot manipulator. IOP Conf Ser Mater Sci Eng. 2018;342(1):012015.

[18] Sun N, Zhang Y. Trajectory tracking control of a 3-DOF robot using improved adaptive sliding mode control. IEEE Access. 2020;8:108500-10.

[19] Boukhnifer M, Benallegue A. Adaptive LQR control for trajectory tracking of a 3-DOF robotic arm. Int J Rob Autom. 2014;29(2):125-34.

[20] Chang CM. Robust control of a 3-DOF robot manipulator using a combined LQR and fuzzy logic control. J Control Sci Eng. 2021;2021:5521990.